HHS Public Access

Author manuscript

Gastroenterology. Author manuscript; available in PMC 2026 July 07.

BIRC3 (encoding cIAP2) variants result in dysregulated RIPK1 signaling leading to increased epithelial cell death and are associated with Monogenic Crohn's Disease

Qi Li[1,*], **Ryusuke Nambu**[1,2,*], **Hu Yaqiang**[3,*], **Xiang Shen**[4,*], **Carmen Argmann**[5,*], **Rei Guan**[1,*], **Erin Janssen**[6,*], **Tom Le Voyer**[7,8,9,*], **Neil Warner**[1], **Daniel D. Yu**[1], **Jing Guo**[1,10], **Kelvin Long**[1], **Jodie Ouahed**[11], **Michael Field**[11], **Lauren Collen**[11], **Jonas Bibus**[4], **David Illig**[4], **Meino Rohlfs**[4], **Ziqi Yu**[4], **Shaohong Yang**[12], **Wenjuan Li**[1], **Craig D. Platt**[13], **Phillip H. Comella**[5], **Daniel Jordan**[5], **Mayte Suárez-Fariñas**[5], **Mohammed F. Alosaimi**[14], **Lauren A. Peters**[5], **Jeremie Rosain**[8,9,15], **Claire Fieschi**[7], **Anne Puel**[8,9], **Elena W. Y. Hsieh**[16,17], **Takeo Naito**[18], **Zhiyang Zeng**[19], **Marta Velasco Rodríguez-Belvís**[20], **Laura Palomino**[20], **Peter Küster**[21], **Dalin Li**[12], **Christoph Klein**[4,22], **Scott B. Snapper**[11,23], **Jean-Laurent Casanova**[8,9,24,25], **Raif Geha**[13], **Edward Hoffenberg**[26], **Dermot P. B. McGovern**[12,**], **Eric Schadt**[5,**], **Daniel Kotlarz**[4,22,27,**], **Dali Li**[3,**], **Aleixo M. Muise**[1,28,**]

[1.]Cell and Systems Biology Program, Research Institute, Hospital for Sick Children, Toronto, Canada

[2.]Center for Pediatric Inflammatory Bowel disease, Division of Gastroenterology and Hepatology, Saitama Children's Medical Center, Saitama, Japan

[3.]Shanghai Frontiers Science Center of Genome Editing and Cell Therapy, Shanghai Key Laboratory of Regulatory Biology, East China Normal University, China

[4.]Dr. von Hauner Children's Hospital, Department of Pediatrics, University Hospital, Ludwig-Maximilians-Universität Munich, Munich, Germany

[5.]Department of Genetics & Genomic Sciences, Icahn School of Medicine at Mount Sinai, New York, USA

Corresponding authors contact information: Dali Li, PhD, Shanghai Frontiers Science Center of Genome Editing and Cell Therapy, Shanghai Key Laboratory of Regulatory Biology and School of Life Sciences, East China Normal University, Shanghai Academy of Natural Sciences (SANS), Shanghai, China. dlli@bio.ecnu.edu.cn, Daniel Kotlarz, PhD, Dr. von Hauner Children's Hospital, Department of Pediatrics, University Hospital, LMU Munich, Munich, Germany. daniel.kotlarz@med.uni-muenchen.de; Institute of Translational Genomics, Helmholtz Zentrum München, German Research Center for Environmental Health, Neuherberg, Germany; German Center for Child and Adolescent Health (DZKJ), partner site Munich, Munich, Germany. [#]**Lead Corresponding authors contact information:** Aleixo M. Muise MD, PhD, 555 University Ave., The Hospital for Sick Children, Toronto, ON, Canada, M5G 1X8, aleixo.muise@utoronto.ca, Fax: 416-813-6531.

Author contributions to manuscript: **Author contributions to manuscript**: QL, RN, HY, JG, XS, CA, RG, EJ, TLV, NW, KL, JO, MF, SY, ZZ, CP, LAP, TN, DL, MF, JB, DI, and ZY carried out experiments and/or analysis under the supervision of JLC, JR, CF, AP, CK, SBS, RG, DPBM, ES, DK, DLL, and AMM. EH, MFA, EH, MVRB, LP, and PK provided clinical care and interpretation of clinical testing, imaging, or pathology. QL, RN, HY, XS, CA, RG, EJ, DPBM, ES, DK, DLL, and AMM wrote the manuscript with contributions from all authors. All authors approved and edited the final draft.

[*]Equal contribution,

[**]Co-senior authorship

Conflict of interest statement: No author has a conflict of interest with regards to the studies carried out in this manuscript.

[6]Division of Pediatric Rheumatology, Michigan Medicine, Ann Arbor, USA

[7]Clinical Immunology Department, Saint Louis Hospital, Paris, France.

[8]Laboratory of Human Genetics of Infectious Diseases, Necker Branch, INSERM, and Imagine Institute, Paris Cité University, Paris, France

[9]St. Giles Laboratory of Human Genetics of Infectious Diseases, Rockefeller Branch, The Rockefeller University, New York, NY, United States.

[10]Department of Pediatrics, Shengjing Hospital of China Medical University, Shenyang, Liaoning, P.R. China

[11]Division of Gastroenterology, Hepatology, & Nutrition, Department of Pediatrics, Boston Children's Hospital, Harvard Medical School, Boston, USA

[12]F. Widjaja Foundation Inflammatory Bowel Research Institute, Cedars-Sinai Medical Center, Los Angeles, USA

[13]Division of Immunology, Department of Pediatrics, Boston Children's Hospital, Harvard Medical School, Boston, USA

[14]College of Medicine, King Saud University, Riyadh, Saudi Arabia

[15]Study Center for Immunodeficiencies, Necker Hospital for Sick Children, Paris, France.

[16]Division of Allergy and Immunology, Departments of Pediatrics and Internal Medicine, Children's Medical Center Dallas, University of Texas Southwestern, Texas, USA

[17]Department of Immunology, University of Texas Southwestern, Texas, USA

[18]Division of Gastroenterology, Tohoku University Graduate School of Medicine, Sendai, Japan

[19]Fengxian Central Hospital Affiliated to Southern Medical University, Shanghai 201499, China.

[20]Sección de Gastroenterología y Nutrición Pediátrica, Hospital Infantil Universitario Niño Jesús, Madrid, Spain

[21]Clemens hospital GmbH Münster, Department of Paediatrics, Munster, Nordrhein-Westfalen, Germany

[22]German Center for Child and Adolescent Health (DZKJ), Munich Site, Munich Germany

[23]Division of Gastroenterology, Hepatology, and Endoscopy, Brigham & Women's Hospital, Harvard Medical School, Boston, USA

[24]Department of Pediatrics, Necker Hospital for Sick Children, AP-HP, Paris, France.

[25]Howard Hughes Medical Institute, New York, NY, United States.

[26]Department of Pediatrics, Children's Hospital Colorado, University of Colorado Anschutz Medical Campus, Colorado, USA

[27]Institute of Translational Genomics, Helmholtz Zentrum München, German Research Center for Environmental Health, Neuherberg, Germany

[28]Departments of Pediatrics, IMS, and Biochemistry, University of Toronto, Toronto, Canada

Abstract

Background and Aims: Tumor Necrosis Factor (TNF) is a key driver of intestinal epithelial inflammation. The baculoviral IAP repeat-containing 3 (*BIRC3*) gene encodes the Cellular Inhibitor of Apoptosis Protein 2 (cIAP2), a known regulator of TNF-signaling. While genetic variants in components of the TNF signalling pathway have been reported, no human *BIRC3* variants have been previously identified.

Methods: We screened exomes obtained from Crohn's disease (CD) patients from multiple centers for *BIRC3* variants. We used cellular, mouse organoids, induced pluripotent stem cells (iPSC)-derived intestinal organoids, knock-in and knock-out mouse models, and knock-out zebrafish, as well as transcriptome analysis of various samples to determine pathogenicity of *BIRC3* variants.

Results: Rare and damaging *BIRC3* variants were identified in 14 patients from 10 unrelated families with CD diagnosed between infancy and adulthood. Functional studies showed that *BIRC3* deficiency caused impaired RIPK1 ubiquitylation leading to RIPK1 autophosphorylation resulting in increased epithelial cell death. The p.H312Y cIAP2 variant identified in both our index and another independent patient was mislocalizaed and a knock-in mouse model of this *BIRC3* variant (cIAP2$^{H312Y/+}$) had exacerbation of chemically induced colitis, while ciap1$^{-/+}$ zebrafish developed spontaneous colitis. Transcriptome analysis of mice organoids and zebrafish showed that *BIRC3* deficiency led to inappropriate sustained activation of TNF-responsiveness genes in the absence of stimuli. Small molecule pharmacological inhibition of RIPK1 or caspases attenuated intestinal inflammation in *BIRC3*-deficient intestinal organoids and cIAP2$^{H312Y/+}$ mice.

Conclusions: We establish *BIRC3*-deficiency as a cause of monogenic CD in both pediatric- and adult-onset patients and identify RIPK1 as a therapeutic target.

Graphical Abstract

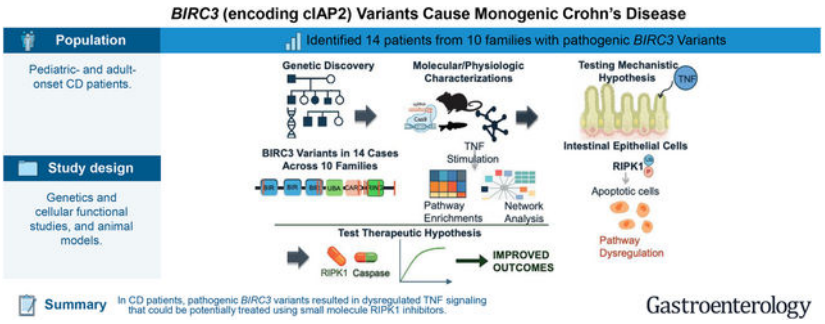

Lay Summary:

We use genetic approaches and preclinical models to identify the disease mechanisms in a single gene responsible for intestinal disease and provide insights how this may change therapy for common Crohn's Disease.

Keywords

Inflammatory Bowel Disease; monogenic IBD; RIPK1; Precision Treatment

Crohn's disease (CD), a form of inflammatory bowel disease (IBD), is characterized by chronic relapsing and remitting disease course with transmural inflammation affecting any part of the gastrointestinal tract. The worldwide prevalence of CD continues to increase across all age groups, including children and adolescents, placing significant burden on health care systems in industrialized, newly industrialized and emerging regions[1]. In IBD, Tumor Necrosis Factor alpha (TNF) is a key driver of intestinal epithelial inflammation. In rare cases, CD can result from pathogenic variants[2–4] in genes encoding regulators of TNF signalling, including *RIPK1*[5–7], *CASP8*[8], *IKBKG* (*NEMO*)[9], and *BIRC4*[10].

Inhibitors of apoptosis (IAPs) are a highly conserved family of Baculoviral IAP repeat-containing genes that in mammalians include *BIRC2* and *BIRC3* (encoding the cellular IAPs, cIAP1 and cIAP2 respectively), and *BIRC4* (encoding X-linked IAP, XIAP). These IAPs are critical signaling molecules that regulate programmed cell death. While cIAP1 and cIAP2 both have putative roles in mediating TNF signaling (reviewed in[11, 12]), cIAP2 is also inducible and regulates innate immune inflammatory responses and cIAP2 knockout mice exhibit resistance to lipopolysaccharide-induced sepsis due to macrophage apoptosis[13]. Previous studies have demonstrated that mice expressing enzymatically inactive cIAP1/2 died during embryonic development due to dysregulated RIPK1-mediated apoptosis[14] and cIAP2-deficient mice exhibit increased susceptibility to chemically induced colitis[15, 16].

While biologics, such as anti-TNF antibodies, and small molecules are now standard treatment for CD[17], these therapies are typically selected empirically rather than being tailored to a patient's specific molecular defect. However, the identification of monogenic causes of intestinal disease has resulted in novel targeted therapeutic options for patients[18–21]. Here, we describe pediatric- and adult-onset CD patients with pathogenic *BIRC3* variants leading to dysregulated TNF signaling, and identity RIPK1 inhibition as a small molecule targeted therapy.

Methods

Study participants

Written informed consent was obtained from participants and/or their guardians in accordance with local regulations in Germany, France, and the United States of America (USA), with approval from the appropriate institutional review boards (IRBs).

Animal Studies

All animal studies followed the ARRIVE guidelines.

Generation of cIAP2$^{H312Y/+}$ and cIAP2$^{-/-}$ Mouse Models

We generated the knock-in cIAP2$^{H312Y/+}$ mice (equivalent to the H312 variant in human cIAP2) and knockout cIAP2$^{-/-}$ mice (as a result of a one nucleotide deletion at amino acid position 313, resulting in a frameshift and premature stop codon at amino acid position 375) by microinjection of Cas9 mRNA, sgRNA, and ssODNs (GenScript, Nanjing, China) into zygotes as described previously[22, 23]. Briefly, super ovulated C57BL/6J female mice were mated with male mice, and one-cell embryos were collected from oviducts. Cas9 mRNA

(50 ng/ul), sgRNA targeting the cIAP2 loci (50 ng/ul), and ssODN (10 ng/ul) carrying the desired point variants were co-injected into the pronuclei of the embryos. The injected embryos were cultured in KSOM before they were transplanted into pseudo-pregnant mice. Two weeks after birth, genomic DNA from the tail of the newborn F0 mice was extracted for sequencing. Mice were housed in standard cages in a specific pathogen-free facility on a 12-h light/dark cycle with ad libitum access to food and water.

Generation of ciap1$^{-/+}$ Zebrafish Model

To generate ciap1$^{-/+}$ mutant zebrafish as previously described[4]. Briefly, gRNA (AACATGCCAAGTGGTTTCCA) was designed on CHOPCHOP[24], and synthesized using the HiScribe T7 High Yield RNA Synthesis Kit (E2040L, New England Biolabs (NEB)), following the manufacturer's instructions. Cas9 mRNA was in vitro synthesized from pT3TS-nCas9n plasmid (a gift from Wenbiao Chen, Addgene, Cat# 46757) using the mMESSAGE mMACHINE™ T3 Transcription Kit (Invitrogen, Cat#AM1348), following the manufacturer's instructions. Next, each AB embryo was injected with 100 pg of gRNA, 150 pg of Cas9 mRNA and 20% phenol red. Once the F0 fish reached adulthood, they were outcrossed to AB to screen for potential founders.

Differentiation of iPSC into Colon Organoids

Human induced pluripotent stem cells (iPSCs) were generated by the iPSC core facility at the German Research Center for Environmental Health (supplementary methods).

RNA-seq Differential Gene Expression Analysis of Mouse Intestinal Organoids

Transcriptomic data was generated on two independent experiments, (either triplicate or duplicate measures per condition) for a total of 30 samples, with 29 remaining after quality control. Genomic alignment of paired-end RNAseq reads to the GRCm38 reference genome was performed using HISAT2 with default parameters. Gene-level quantification was conducted using featureCounts, also with default settings. Multimapping reads were flagged and discarded. Genes with low expression were filtered using edgeR's filterByExpr() function based on the experimental design prior to normalization and linear modeling. After filtering, count data was normalized via the weighted trimmed mean of M-values[25]. Normalized counts were transformed via the voom-transformation and was the final input for statistical modeling. Statistical analysis was carried out using Limma framework[26, 27] in R language version 4.3.3 and its available packages as described previously[28] and in supplementary methods

RNA-seq Differential Gene Expression Analysis in Zebrafish

Human orthologs of Zebrafish differentially expressed genes were determined using DRSC integrative ortholog prediction tool (DIOPT v8.5/ 9.0)[29]. Multi-mapped genes were removed and only high ranking orthologs kept. At Adj $P<0.05$, 116 down and 305 up-regulated DEGs were identified and after converting to human orthologs we identified 71 down and 210 up-regulated genes.

Gene Set Enrichment Analysis

Enrichment analyses were done using the Fisher's exact test (FET, unless otherwise stated) with p-values adjusted using a Benjamini Hochberg ((BH) multiple test correction (significant if adj $p < 0.05$) procedure. Geneset enrichment analysis (GSEA[30]) was also performed using GSEA software (v4.3.2) and the pre-ranked function (t statistic) with 1000 permutations. Canonical pathways included Hallmark (v2023.2.Hs.symbols); and Reactome (v2022). Genesets related to IBD GWAS[31], monogenic IBD genes[32], anti-TNF response vs non-response[33, 34] were curated from cited resources. As indicated, either normalized enrichment scores (NES) or significance was presented in heatmap (negative log adjusted P value) using the R package pheatmap or dot plot using R package ggplot2[35].

Network Analysis

Bayesian Gene Regulatory Networks (BGRNs) can capture fundamental properties of complex systems in states that give rise to complex (diseased) phenotypes[36]. BGRNs were generated as previously reported[28] from colonic biopsy RNA sequence data (Mount Sinai Crohn's and Colitis Registry (MSCCR) CD subset using intestinal expression QTL information as priors[37]). The network included both inflamed and uninflamed biopsies and was constructed using RIMBAnet software[38] and visualized using Cytoscape 3.7[39]. To evaluate the BIRC3-centered subnetwork in the context of anti-TNF therapy, we quantified activity of the subnetwork (GSVA R package) in gut transcriptomic data from the ACT1 infliximab (IFX) clinical trial in adult ulcerative colitis (GSE23597)[34] and compared levels between IFX responders vs non-responders (see Supplementary methods).

Functional Assay

Several functional assays were used and outlined in the Supplemental Material.

Results

Identification of *BIRC3* variants in Crohn's Disease patients.

Exome sequencing of our index patient (patient 4), a young boy who presented with typical CD features (oral ulcers, perianal disease, and granulomatous ileo-colonic inflammation) identified a heterozygous de novo *BIRC3* variant (NM_001165: c.934C>T) that resulted in a novel cIAP2 p.H312Y protein not reported in any database (Figure 1A; Table 1). Subsequent screening of CD patients for rare *BIRC3* variants revealed 13 additional individuals from 9 unrelated families (diagnosed between < 1 to 31 years of age), including patient 5 who presented at 12 years of age and carried the same heterozygous p.H312Y cIAP2 variant as the index proband. While pediatric- or adult-onset CD patients carried heterozygous cIAP2 variants (p.T35A, p.P266R, p.H312Y, p.C557X, and p.D530H), three sibling pairs from independent consanguineous families harbored homozygous cIAP2 variants (p.Y522X, p.C588Y, and p.X605Rext10) and presented in infancy (Figure 1B). All *BIRC3* variants were localized to highly conserved regions (Figure 1C), rare (novel or gnomAD[40] allele frequency < 0.00001), damaging (Combined Annotation Dependent Depletion (CADD) Score[41] > 15) and classified as either likely pathogenic or as variants of unknown significance based on the ACMG/AMP classification[42] (Table 1).

CD-associated cIAP2 variants result in dysregulated RIPK1-dependent cell death in intestinal epithelial cells

To determine the functional significance of the identified cIAP2 variants in TNF signaling, we overexpressed all the cIAP2 variants in human embryonic kidney (HEK293T) cells. Upon TNF stimulation, all cIAP2 variants exhibited increased apoptosis as measured by elevated CASP3/7 levels using a Caspase-Glo®3/7 assay (Figure 2A). Furthermore, overexpression of the cIAP2 variants in HEK293T cells resulted in reduced RIPK1 ubiquitylation when stimulated with TNF (Figure 2B) and serine 166 (S166) RIPK1 autophosphorylation when co-stimulated with TNF and the SMAC mimetic BV6 (Figure 2C) compared to wildtype cIAP2. To further model the patient-specific effects in a physiologically relevant model, we generated CRISPR-engineered human iPSC-derived intestinal organoids with either cIAP2 knock-out (cIAP2$^{-/-}$) or knock-in of several patient variants (H312Y, Y522X, and X605Rext10; Figure 2D), as well as the cIAP2 KO HCT116 cells and reconstituted them with overexpression of the above-mentioned variants. Similar S166 RIPK1 autophosphorylation was observed in these human iPSC-derived intestinal organoids (Figure 2D) and HCT116 cells (Figure S1A) expressing either cIAP2 knock-out (cIAP2$^{-/-}$) or knock-in of the patient-associated cIAP2 variants upon co-stimulation with TNF/BV6. In support of cIAP2's role in regulating RIPK1-dependent signalling, after TNF treatment, qPCR analysis showed elevated expression of pro-inflammatory *CCL5* and *CCL20* chemokines in HCT116 cells with knock-out of cIAP2 or lentiviral knock-in of several patient-associated cIAP2 variants compared to wildtype (Figure S1B). Furthermore, we demonstrate that overexpression of all patient-associated cIAP2 variants increased *CCL20* in HEK293T cells upon TNF stimulation (Figure S1C). Co-transfection of WT cIAP2 in HEK293T cells overexpressing all the patient-derived variants demonstrated a dose-dependent partial rescue of apoptosis as measured by Caspase3/7 activity after TNF treatment indicating loss-of-function rather than a dominant-negative effect (Figure 2E). Furthermore, in HeLa cells, the H312Y, T35A, and X605Rext*10 cIAP2 variants under TNF/BV6 stimulation exhibited distinct punctate indicating a trafficking defect may be responsible for the loss-of-function for these cIAP2 variants (Figure 2F).

cIAP2$^{H312Y/+}$ mice and ciap1$^{+/-}$ zebrafish exhibit inflammation with enhanced intestinal epithelial apoptosis.

To further investigate the effects of the patient-associated *BIRC3* variants on intestinal inflammation, we generated CRISPR-engineered zebrafish and mouse knock-out models, as well as a knock-in mouse model harboring the (cIAP2$^{H312Y/+}$) equivalent to the human heterozygous cIAP2 p.H312Y protein variant identified in two independent families with CD (see Methods and Figure S2A–D). cIAP2$^{H312Y/+}$ mice showed no overt intestinal abnormalities and were phenotypically indistinguishable from wildtype cIAP2$^{+/+}$ littermates (Figure S2E). However, when challenged with 3% dextran sulfate sodium (DSS), the cIAP2$^{H312Y/+}$ mice developed exacerbated colitis as evidenced by increased disease activity index and shortened colon length when compared to cIAP2$^{+/+}$ wildtype littermates (Figure 3A). Histopathological examination using hematoxylin and eosin (H&E) stained colon sections showed severe intestinal inflammation in cIAP2$^{H312Y/+}$ mice, including distortion of tissue architecture, infiltration of inflammatory cells, edema in the lamina propria area, as well as apoptotic cells throughout the colon and small intestine (Figure 3B). Consistent with

increased epithelial cell death, cleaved CASP3 staining was markedly elevated throughout the intestine of DSS-treated cIAP2$^{H312Y/+}$ mice (Figure 3C and D). Of note, our index patient 4 with the p.H312Y cIAP2 variant also exhibited increased apoptosis in intestinal biopsies (Figure 1A).

In contrast to mice and humans, zebrafish possess a single cellular *birc* gene (*birc2* encoding ciap1)[43], an orthologue of both human *BIRC2* and *BIRC3* genes. Knock-out of *birc2* in zebrafish (ciap1$^{-/-}$) resulted in lethality within four days post-birth, whereas heterozygous ciap1$^{-/+}$ zebrafish survived but developed spontaneous intestinal inflammation in adulthood. Histological analysis (H&E and alcian blue staining) of the ciap1$^{-/+}$ zebrafish showed epithelial damage, infiltration of inflammatory cells, and loss of architecture as compared to ciap1$^{+/+}$ zebrafish (Figure 3E–F). Additionally, immunofluorescence revealed increased casp8 staining in the intestinal epithelium of adult ciap1$^{-/+}$ zebrafish, indicating increased cell death (Figure 3G).

Integrative molecular analysis identifies *BIRC3* as a driver of TNF-associated transcriptional activation and altered TNF responsiveness

To define the transcriptional consequences of cIAP2 perturbation, RNA sequencing was performed on mouse intestinal organoids derived from cIAP2$^{+/+}$ (WT), cIAP2$^{H312Y/+}$, and cIAP2$^{-/-}$ mice under basal conditions and following TNF stimulation. In unstimulated conditions, cIAP2$^{-/-}$ organoids exhibited widespread differential gene expression (DEG) relative to WT (Figure 4A; Tables ST1–2). The cIAP2$^{H312Y/+}$ organoids displayed a similar but attenuated transcriptional profile with significant DEGs strongly enriched within the cIAP2$^{-/-}$ DEG set (Fold Enrichment (FE) 3.9, $P = 6.8 \times 10^{-05}$; Table ST3).

Direct comparison of basal cIAP2$^{-/-}$ and cIAP2$^{H312Y/+}$ log2 fold changes demonstrated moderate concordance in transcriptional directionality (Pearson $r = 0.36$, $P < 2 \times 10^{-16}$; Figure 4B), indicating a shared biological program. Linear regression across all genes yielded a slope of 0.28, indicating that heterozygous organoids retain approximately 28% of the transcriptional amplitude observed in knockout organoids suggesting a gene dosage–dependent hypomorphic phenotype. We observed that untreated organoids from cIAP2$^{H312Y/+,}$ and cIAP2$^{-/-}$ mice effectively mimicked the DEGs from TNF stimulated cIAP2$^{+/+}$ organoids with approximately 35% of TNF-stimulated genes in WT organoids already induced in untreated cIAP2$^{-/-}$ organoids (FE of 3.35, $P = 1.5 \times 10^{-94}$, Table ST3). Gene set enrichment analysis (GSEA) using the TNF stimulated cIAP2$^{+/+}$ organoids up-regulated gene set confirmed significant enrichment in both cIAP2$^{-/-}$ and cIAP2$^{H312Y/+,}$ organoids (Figure 4C, Table ST4), indicating constitutive activation of TNF-responsive pathways in the absence of stimulation.

Upon TNF stimulation, both cIAP2$^{-/-}$ and cIAP2$^{H312Y/+}$ organoids induced TNF-responsive gene signatures, as reflected by strong positive normalized enrichment scores (NES, Figure 4C, Table ST4). However, interaction modeling comparing TNF responses in cIAP2 models relative to cIAP2$^{+/+}$ organoids demonstrated a general blunted TNF effect (Figure 4C–D; Table ST1). Interaction volcano plots revealed impaired amplification of TNF signaling in the context of reduced cIAP2 activity. These findings suggest that while cIAP2 deficiency creates a chronically primed inflammatory state, it simultaneously reduces the dynamic

range of acute TNF responsiveness. Consistent with this pattern, Hallmark pathway analysis showed that inflammatory, interferon-γ, IL6–JAK–STAT3, and apoptosis-related programs were induced in cIAP2$^{-/-}$ organoids under basal and upon TNF treatment but showed reduced enrichment in the differential TNF treatment comparisons (Figure 4E, Table ST5). These pathways were also enriched in DEGs identified from RNA sequence analysis of ciap$^{-/-}$ zebrafish compared to wildtype ciap$^{+/+}$ controls, validating the mouse organoid findings and confirming that reduced or absent cIAP2 expression generates a gene expression signature closely resembling TNF stimulation (Tables ST6–7). Furthermore, the gene level analysis revealed several candidate genes important in RIPK1-dependent cell death pathways, including the up-regulation of casp8 in the ciap1$^{-/-}$ zebrafish; and the up-regulation (<FDR0.05) of Casp3, Nfkb2, Cflar (encoding cFLIP) and Tnfsf10 in the cIAP2$^{-/-}$ mice organoid model (Tables ST1 and 7). Interestingly, we noted several metabolic pathways (e.g. Cholesterol Homeostasis, Fatty Acid Metabolism and Glycolysis) displayed altered baseline regulation in cIAP2$^{-/-}$ organoids with divergent responses upon TNF stimulation. As these metabolic programs were not strongly induced by TNF in cIAP2$^{+/+}$ organoids, their basal activation represents a consequence of cIAP2$^{-/-}$ deficiency rather than TNF stimulation per se.

To understand the relevance of cIAP2 deficiency beyond Mendelian CD, we next contextualized *BIRC3* within regulatory programs active in adult Crohn's disease (CD). We leveraged a large Bayesian regulatory network constructed from mucosal transcriptomic profiles of approximately 400 adult CD patients representing both active and inactive disease states (MSCCR cohort[37]). From this framework, we extracted a *BIRC3*-centered subnetwork encompassing regulatory interactions spanning up to four path lengths from *BIRC3*, yielding ~500 connected genes (Figure 4F, Table ST8). This *BIRC3*-centric neighborhood was significantly enriched for multiple independent IBD-relevant gene signatures (Figure 4G, Table ST9). These included genes upregulated during active intestinal inflammation, genes located within IBD GWAS[31], and monogenic IBD genes[32]. Notably, the subnetwork was also enriched for transcriptional programs induced by *BIRC3* perturbation across cIAP2$^{-/-}$ model systems, including zebrafish and murine organoid models under basal and TNF-stimulated conditions, supporting the predicted *BIRC3* regulatory interactions in adult gut. Network topology revealed close connectivity of *BIRC3* with key inflammatory regulators, including *NFKB2* and its downstream effector *CCL20*, as well as central mediators of apoptosis and TNF signaling such as *TNFAIP3*.

Notably, the *BIRC3* subnetwork demonstrated strong enrichment for TNF-responsive gene programs and was significantly overrepresented among genes differentially expressed in anti-TNF non-responders compared to responders across adult IBD cohorts[33, 34]. To further evaluate the clinical relevance of this network, we calculated a gene set variation analysis (GSVA) score for the *BIRC3*-centered subnetwork in longitudinal mucosal biopsy samples from infliximab-treated patients in the ACT1 cohort[34]. At baseline, responders and non-responders exhibited comparable subnetwork activity. However, by week 30 of infliximab therapy, responders demonstrated a significantly greater reduction in *BIRC3* mRNA as well as the *BIRC3* subnetwork GSVA score compared to non-responders (Figure S3, Table ST10). In contrast, non-responders showed persistent subnetwork activation despite therapy. Interestingly, the genotype-interaction-associated programs largely mapped to metabolic and

stress-response modules outside the immediate *BIRC3*-centered inflammatory subnetwork suggesting *BIRC3* deficiency exerts dual effects. Overall, our findings support a model in which cIAP2 deficiency primes epithelial cells toward a constitutive inflammatory state and metabolically activated basal state while constraining dynamic responsiveness during TNF challenge, revealing reduced signaling flexibility.

Pharmacologic inhibition of RIPK1 and caspases attenuates inflammation and cell death in cIAP2-deficient models

To explore potential therapeutic strategies for patients with dysregulated cIAP2-associated CD, we tested for enrichment in molecular signatures of birinapant[44], a SMAC mimetics targeting cIAP1/2 and XIAP used in clinical cancer trials, and necrostatin-1[45] (Nec-1), a small molecule RIPK1 inhibitor, curated from the LINCs L1000 chemical perturbation consensus database[46]. The gene signatures induced by birinapant closely resembled the transcriptional effects observed in ciap1-deficient zebrafish and cIAP2-deficient mouse organoids. In contrast, gene expression signatures induced by Nec-1 treatment were significantly enriched among DEGs from cIAP2-knockout models but largely in the opposing direction, suggesting a potential therapeutic target for these patients with *BIRC3* variants (Table ST11).

Live-cell imaging of human iPSC-derived intestinal organoids revealed increased cell death with either cIAP2 knock-out (cIAP2$^{-/-}$) or knock-in of several patient cIAP2 variants following treatment with TNF and the SMAC mimetic BV6 compared to wild-type controls. However, treatment with either Z-VAD-FMK[47], a pan-caspase inhibitor, or Nec-1 markedly reduced Draq7 signal, indicating that both inhibitors conferred protection against TNF-induced cell death (Figure 5A). Similar protective effects were seen in HCT116 cells with cIAP2 knock-out or lentiviral knock-in overexpression of several patient variants (Figure S4). Finally, we evaluated these potential therapeutic small molecule inhibitors using our cIAP2$^{H312Y/+}$ mouse model. Intraperitoneal injection of either Z-VAD-FMK or Nec-1 reduced colonic inflammation in DSS-treated cIAP2$^{H312Y/+}$ mice as indicated by reduced disease activity index and improved histopathology compared to untreated cIAP2$^{H312Y/+}$ mice littermates (Figure 5B).

Discussion

We describe 8 germline *BIRC3* genetic variants identified in 14 people with CD from 10 families diagnosed between infancy and adulthood and presenting with typical features of colonic or ileocolonic CD. Knock-in cIAP2$^{H312Y/+}$ mice and heterozygote ciap1$^{-/+}$ zebrafish recapitulated key features of the human intestinal phenotype, including intestinal inflammation with epithelial apoptosis. The experimental and molecular data demonstrate that all 8 *BIRC3* genetic variants resulted in reduced cIAP2 protein function that could be rescued by wildtype cIAP2 (Mechanism is outline in Figure 6). Another important finding is that identified *BIRC3* variants were either autosomal dominant (AD) or autosomal recessive (AR) indicating mixed inheritance. As expected, the AR variants (3 independent consanguineous families harbored homozygous cIAP2 variants (p.Y522X, p.C588Y, and p.X605Rext*10)) resulted in a stronger phenotype with early diagnosis of CD (infancy) and

several extraintestinal manifestation of disease including fever, skin and joint inflammation. Whereas the AD variants presented as older children and adults with typical CD features. Therefore, we believe the AR and AD inheritance strengthens the findings and suggests a broader role of cIAP2 in CD pathogenesis. However, with the wide age range of disease onset, even within families, the identification of additional CD patients with *BIRC3* variants and complete familial genotyping is required to determine the disease penetrance and if there is variable expressivity in CD phenotypes. Similarly, variants in several genes involved in regulating TNF-signaling including *NFKB1*[48], *RelA*[49], *OTULIN*[50], and *TNFAIP3*/A20[51] result in haploinsufficiency and *OTULIN*-deficieny[50] has both an AR and AD mixed inheritance pattern similar to what we describe here for *BIRC3*. Moreover, incomplete penetrance and variable expressivity is commonly described in patients with both mono-allelic and bi-allelic TNF-signalling defects (reviewed in[52]).

While 8 patients from 7 independent families had missense *BIRC3* variants, 6 patients from 3 independent families had *BIRC3* variants that resulted in premature termination codons (PTCs). Two of the 3 *BIRC3* PTC variants were located in the final exon, and 1 PTC variant was in the penultimate exon less than 50 nucleotides upstream from the exon-exon junction; therefore, these transcripts would be expected to escape nonsense mediated decay[53] and express truncated cIAP2 proteins. As we have shown here, these truncated proteins cause reduced, but not complete loss, of cIAP2 protein function. Multi-system transcriptomic analyses reveal that cIAP2 functions as a dosage-sensitive regulator of TNF signaling, shaping inflammatory activation, metabolic adaptation, and epithelial survival. This integrative framework links *BIRC3*-deficiency to both Mendelian intestinal disease and broader TNF-dependent inflammatory pathways in human IBD.

BIRC3-deficiency results in CD without the significant immunodeficiency and systemic disease that is associated with other TNF-signalling defects, suggesting a specific role for cIAP2 in the intestinal epithelium homeostasis. Mechanistically, the patient-derived cIAP2 variants impaired RIPK1 ubiquitylation, resulting in increased RIPK1 autophosphorylation and cell death upon challenge with TNF. RNA sequencing analysis demonstrated that reduced cIAP2 resulted in constitutive activation of TNF signaling pathways and a blunted response to TNF stimulation. Furthermore, the patient-derived cIAP2 variants increased the expression of *CCL5* and *CCL20* chemokines, suggesting that cIAP2-deficiency may also lead to the infiltration of immune cells into the intestine. Co-enrichment of *BIRC3* with TNF responder vs non-responder genes in the adult CD subnetwork suggested a broader relevance of *BIRC3* expression beyond Mendelian disease in polygenic CD. While cIAP1 and cIAP2 both have putative roles in mediating TNF signaling (reviewed in[11, 12]), we demonstrate that in intestinal epithelium, cIAP2 has a distinct role in regulating TNF response. While our studies primarily focused on the role of cIAP2 in maintaining intestinal homeostasis, it is possible that non-epithelial cells, including immune cells, as well as other non-apoptotic cellular pathways contributes to disease pathogenesis. Previous studies have demonstrated that enzymatically inactive cIAP1/2 mice died during embryonic development due to dysregulated RIPK1-mediated apoptosis[14] and cIAP2 deficient mice exhibit increased susceptibility to chemically induced colitis[15, 16]. cIAP1$^{-/-}$ mice with inducible knockout of cIAP2 die within three days, exhibiting overt inflammation and apoptosis in the intestine and liver, primarily driven by caspase 8[54]. Together, this implies complex regulation of

cIAP1 and cIAP2, and that further study of cIAP2 regulation, specifically in human disease, will provide insight into not only the immune regulation of inflammation but also CD pathogenesis.

Conventional IBD treatment strategies often fail to achieve sustained remission highlighting the need for targeted therapeutic approaches and yet there is still no molecular rationale for the selection of specific biologics or small molecules. Our study reveals an essential and protective role of cIAP2 in regulating TNF-mediated cell death and intestinal injury. Dysregulation of TNF-responsive gene expression in polygenic CD, suggest that modulating pathways disrupted by loss of cIAP2 could offer new therapeutic strategies for CD patients. To this point, we showed the therapeutic potential of a pan-caspase inhibitor (Z-VAD-FMK) and RIPK1 inhibitor (Nec-1) in human iPSC-derived intestinal organoids. Furthermore, the administration of these inhibitors in the cIAP2$^{H312Y/+}$ mouse model successfully alleviated key pathological features associated with CD in patients, including intestinal inflammation, epithelial cell damage, and crypt loss. Of note, the RIPK1 inhibitor GSK2982772, a necrostatin-1 analogue, has been evaluated in patients with active ulcerative colitis[55–57]. While GSK2982772 was generally well-tolerated by patients, it did not significantly outperform the placebo. Nevertheless, our study, along with GSK2982772 and ongoing RIPK1 inhibitor clinical trials including GDC-8264[58] and others (ABBV-668 and SAR443122 reviewed in[17]) suggests that RIPK1 is a promising IBD molecular target and stratifying patients (e.g., CD and/or dysregulated TNF signaling) may improve therapeutic outcomes. These results highlight the therapeutic potential of targeting dysregulated cell death pathways through small molecule inhibition of RIPK1 in patients with *BIRC3*-deficiency, other TNF-related forms of monogenic CD, and potentially in a subset of polygenic CD characterized by identifying similar transcriptional profiles.

Supplementary Material

Refer to Web version on PubMed Central for supplementary material.

Acknowledgements:

We thank all the patients and their families for participating in this study and the coordinators as part of the VEOIBD Consortium (www.VEOIBD.org). The generation of zebrafish *birc2* mutant lines and genotyping was performed by Xiucheng Cui and Jason Burgess in Zebrafish Genetics and Disease Models Facility, The Hospital for Sick Children, Toronto, Canada. Yue Li has provided expertise in immunophenotyping of patients with *BIRC3* deficiency.

Funding:

AMM, SBS, CK, DK, ES, CA and DPBM are funded by The Leona M. and Harry B. Helmsley Charitable Trust and AMM, SBS, CK, DK, ES, CA the National Institute of Diabetes and Digestive Kidney Diseases (NIDDK) of the National Institutes of Health (NIH) (RC2DK122532). AMM is funded by NIDDK (RC2DK118640), Canada Research Chair (Tier 1) in Pediatric IBD, and CIHR Foundation Grant. JO and DPBM are supported by NIDDK (award numbers K08DK122133 and U01DK062413 respectively). DLL, YQH, ZZ are funded by the National Natural Science Foundation of China (No.32025023) and grant from the Shanghai Municipal Commission for Science and Technology (No. 24J22800400). DK is also funded by the Deutsche Forschungsgemeinschaft (DFG, German Research Foundation - Projektnummern: Heisenberg grant, KO 4891/6-1, 496078873; KO 4891/5-1, 447562338), Helmholtz Initiative and Networking Fund of the Helmholtz Association (Helmholtz Young Investigator Group, VH-NG-1716), Else Kröner-Fresenius-Stiftung (Key Project 2019_A136), and Care-for-Rare Foundation. XS is funded by China Scholarship Council (201909110092), Klinikum LMU and Care-for-Rare Foundation. ZY is also funded by China Scholarship Council (202008360174) Klinikum LMU and Care-for-Rare Foundation. TLV. is supported by the MD-PhD program of the Imagine Institute (with support from the *Fondation*

Bettencourt-Schueller), and a "*Poste CCA-INSERM-Bettencourt*" (with support from the *Fondation Bettencourt-Schueller*).

Data availability:

The identified *BIRC3* variants have been submitted to the ClinVar database (https://www.ncbi.nlm.nih.gov/clinvar/) with the IDs SCV006100892 - SCV006100899. Human sequencing is not made publicly available as they contain information that could compromise research participant privacy/consent; however, it will be available to researchers upon request. Zebrafish and mice RNA sequencing data is available at public repository – GEO accession GSE299375.

References

1. Hracs L, Windsor JW, Gorospe J, et al. Global evolution of inflammatory bowel disease across epidemiologic stages. Nature 2025;642:458–466. [PubMed: 40307548]
2. Crowley E, Warner N, Pan J, et al. Prevalence and Clinical Features of Inflammatory Bowel Diseases Associated With Monogenic Variants, Identified by Whole-Exome Sequencing in 1000 Children at a Single Center. Gastroenterology 2020;158:2208–2220. [PubMed: 32084423]
3. Nambu R, Warner N, Mulder DJ, et al. A Systematic Review of Monogenic Inflammatory Bowel Disease. Clin Gastroenterol Hepatol 2022;20:e653–e663. [PubMed: 33746097]
4. Gaibee Z, Warner N, Bugda Gwilt K, Li W, Guan R, et al. The Genetic Architecture of Congenital Diarrhea and Enteropathy. N Engl J Med 2025;392:1297–1309. [PubMed: 40174224]
5. Li Y, Fuhrer M, Bahrami E, et al. Human RIPK1 deficiency causes combined immunodeficiency and inflammatory bowel diseases. Proc Natl Acad Sci U S A 2019;116:970–975. [PubMed: 30591564]
6. Tao P, Sun J, Wu Z, Wang J, Li W, et al. A dominant autoinflammatory disease caused by noncleavable variants of RIPK1. Nature 2020;577:109–114. [PubMed: 31827280]
7. Cuchet-Lourenco D, Eletto D, Wu C, et al. Biallelic RIPK1 mutations in humans cause severe immunodeficiency, arthritis, and intestinal inflammation. Science 2018;361:810–813. [PubMed: 30026316]
8. Lehle AS, Farin HF, Marquardt B, et al. Intestinal Inflammation and Dysregulated Immunity in Patients with Inherited Caspase-8 Deficiency. Gastroenterology 2018.
9. Zilberman-Rudenko J, Shawver LM, Wessel AW, et al. Recruitment of A20 by the C-terminal domain of NEMO suppresses NF-κB activation and autoinflammatory disease. Proc Natl Acad Sci U S A 2016;113:1612–7. [PubMed: 26802121]
10. Zeissig Y, Petersen BS, Milutinovic S, et al. XIAP variants in male Crohn's disease. Gut 2014.
11. Lalaoui N, Vaux DL. Recent advances in understanding inhibitor of apoptosis proteins. F1000Res 2018;7.
12. Darding M, Meier P. IAPs: guardians of RIPK1. Cell Death Differ 2012;19:58–66. [PubMed: 22095281]
13. Conte D, Holcik M, Lefebvre CA, et al. Inhibitor of apoptosis protein cIAP2 is essential for lipopolysaccharide-induced macrophage survival. Mol Cell Biol 2006;26:699–708. [PubMed: 16382159]
14. Schorn F, Werthenbach JP, Hoffmann M, et al. cIAPs control RIPK1 kinase activity-dependent and -independent cell death and tissue inflammation. EMBO J 2023;42:e113614. [PubMed: 37789765]
15. Dagenais M, Dupaul-Chicoine J, Champagne C, et al. A critical role for cellular inhibitor of protein 2 (cIAP2) in colitis-associated colorectal cancer and intestinal homeostasis mediated by the inflammasome and survival pathways. Mucosal Immunol 2016;9:146–58. [PubMed: 26037070]
16. Bertrand MJ, Doiron K, Labbe K, et al. Cellular inhibitors of apoptosis cIAP1 and cIAP2 are required for innate immunity signaling by the pattern recognition receptors NOD1 and NOD2. Immunity 2009;30:789–801. [PubMed: 19464198]

17. Vieujean S, Jairath V, Peyrin-Biroulet L, et al. Understanding the therapeutic toolkit for inflammatory bowel disease. Nat Rev Gastroenterol Hepatol 2025;22:371–394. [PubMed: 39891014]
18. Yao Y, Kim G, Shafer S, et al. Mucus sialylation determines intestinal host-commensal homeostasis. Cell 2022.
19. Uhlig HH, Booth C, Cho J, et al. Precision medicine in monogenic inflammatory bowel disease: proposed mIBD REPORT standards. Nat Rev Gastroenterol Hepatol 2023;20:810–828. [PubMed: 37789059]
20. Jardine S, Anderson S, Babcock S, et al. Drug Screen Identifies Leflunomide for Treatment of Inflammatory Bowel Disease Caused by TTC7A Deficiency. Gastroenterology 2020;158:1000–1015. [PubMed: 31743734]
21. Wang L, Aschenbrenner D, Zeng Z, et al. Gain-of-function variants in SYK cause immune dysregulation and systemic inflammation in humans and mice. Nat Genet 2021;53:500–510. [PubMed: 33782605]
22. Li D, Qiu Z, Shao Y, et al. Heritable gene targeting in the mouse and rat using a CRISPR-Cas system. Nat Biotechnol 2013;31:681–3. [PubMed: 23929336]
23. Shao Y, Guan Y, Wang L, et al. CRISPR/Cas-mediated genome editing in the rat via direct injection of one-cell embryos. Nat Protoc 2014;9:2493–512. [PubMed: 25255092]
24. Montague TG, Cruz JM, Gagnon JA, et al. CHOPCHOP: a CRISPR/Cas9 and TALEN web tool for genome editing. Nucleic Acids Res 2014;42:W401–7. [PubMed: 24861617]
25. Robinson MD, Oshlack A. A scaling normalization method for differential expression analysis of RNA-seq data. Genome Biol 2010;11:R25. [PubMed: 20196867]
26. Ritchie ME, Phipson B, Wu D, et al. limma powers differential expression analyses for RNAsequencing and microarray studies. Nucleic Acids Res 2015;43:e47. [PubMed: 25605792]
27. Law CW, Chen Y, Shi W, et al. voom: Precision weights unlock linear model analysis tools for RNAseq read counts. Genome Biol 2014;15:R29. [PubMed: 24485249]
28. Suarez-Farinas M, Tokuyama M, Wei G, et al. Intestinal Inflammation Modulates the Expression of ACE2 and TMPRSS2 and Potentially Overlaps With the Pathogenesis of SARS-CoV-2-related Disease. Gastroenterology 2021;160:287–301 e20. [PubMed: 32980345]
29. Hu Y, Flockhart I, Vinayagam A, et al. An integrative approach to ortholog prediction for diseasefocused and other functional studies. BMC Bioinformatics 2011;12:357. [PubMed: 21880147]
30. Subramanian A, Tamayo P, Mootha VK, et al. Gene set enrichment analysis: a knowledge-based approach for interpreting genome-wide expression profiles. Proc Natl Acad Sci U S A 2005;102:15545–50. [PubMed: 16199517]
31. de Lange KM, Moutsianas L, Lee JC, et al. Genome-wide association study implicates immune activation of multiple integrin genes in inflammatory bowel disease. Nat Genet 2017;49:256–261. [PubMed: 28067908]
32. Bolton C, Smillie CS, Pandey S, et al. An Integrated Taxonomy for Monogenic Inflammatory Bowel Disease. Gastroenterology 2022;162:859–876. [PubMed: 34780721]
33. West NR, Hegazy AN, Owens BMJ, et al. Oncostatin M drives intestinal inflammation and predicts response to tumor necrosis factor-neutralizing therapy in patients with inflammatory bowel disease. Nat Med 2017;23:579–589. [PubMed: 28368383]
34. Toedter G, Li K, Marano C, et al. Gene expression profiling and response signatures associated with differential responses to infliximab treatment in ulcerative colitis. Am J Gastroenterol 2011;106:1272–80. [PubMed: 21448149]
35. Wickham H ggplot2 : Elegant Graphics for Data Analysis. Use R!,. 2nd ed. Cham: Springer International Publishing : Imprint: Springer,, 2016:1 online resource (XVI, 260 pages 232 illustrations, 140 illustrations in color.
36. Peters LA, Perrigoue J, Mortha A, et al. A functional genomics predictive network model identifies regulators of inflammatory bowel disease. Nat Genet 2017;49:1437–1449. [PubMed: 28892060]
37. Argmann C, Hou R, Ungaro RC, et al. Biopsy and blood-based molecular biomarker of inflammation in IBD. Gut 2022.

38. Zhu J, Zhang B, Smith EN, et al. Integrating large-scale functional genomic data to dissect the complexity of yeast regulatory networks. Nat Genet 2008;40:854–61. [PubMed: 18552845]
39. Shannon P, Markiel A, Ozier O, et al. Cytoscape: a software environment for integrated models of biomolecular interaction networks. Genome Res 2003;13:2498–504. [PubMed: 14597658]
40. Karczewski KJ, Francioli LC, Tiao G, et al. The mutational constraint spectrum quantified from variation in 141,456 humans. Nature 2020;581:434–443. [PubMed: 32461654]
41. Rentzsch P, Witten D, Cooper GM, et al. CADD: predicting the deleteriousness of variants throughout the human genome. Nucleic Acids Res 2019;47:D886–D894. [PubMed: 30371827]
42. Richards S, Aziz N, Bale S, et al. Standards and guidelines for the interpretation of sequence variants: a joint consensus recommendation of the American College of Medical Genetics and Genomics and the Association for Molecular Pathology. Genet Med 2015;17:405–24. [PubMed: 25741868]
43. Santoro MM, Samuel T, Mitchell T, et al. Birc2 (cIap1) regulates endothelial cell integrity and blood vessel homeostasis. Nat Genet 2007;39:1397–402. [PubMed: 17934460]
44. Krepler C, Chunduru SK, Halloran MB, et al. The novel SMAC mimetic birinapant exhibits potent activity against human melanoma cells. Clin Cancer Res 2013;19:1784–94. [PubMed: 23403634]
45. Degterev A, Huang Z, Boyce M, et al. Chemical inhibitor of nonapoptotic cell death with therapeutic potential for ischemic brain injury. Nat Chem Biol 2005;1:112–9. [PubMed: 16408008]
46. Evangelista JE, Clarke DJB, Xie Z, Lachmann A, et al. SigCom LINCS: data and metadata search engine for a million gene expression signatures. Nucleic Acids Res 2022;50:W697–W709. [PubMed: 35524556]
47. Zhu H, Fearnhead HO, Cohen GM. An ICE-like protease is a common mediator of apoptosis induced by diverse stimuli in human monocytic THP.1 cells. FEBS Lett 1995;374:303–8. [PubMed: 7589559]
48. Lorenzini T, Fliegauf M, Klammer N, et al. Characterization of the clinical and immunologic phenotype and management of 157 individuals with 56 distinct heterozygous NFKB1 mutations. J Allergy Clin Immunol 2020;146:901–911. [PubMed: 32278790]
49. Badran YR, Dedeoglu F, Leyva Castillo JM, et al. Human RELA haploinsufficiency results in autosomal-dominant chronic mucocutaneous ulceration. J Exp Med 2017;214:1937–1947. [PubMed: 28600438]
50. Davidson S, Shibata Y, Collard S, et al. Dominant negative OTULIN-related autoinflammatory syndrome. J Exp Med 2024;221.
51. Zhou Q, Wang H, Schwartz DM, et al. Loss-of-function mutations in TNFAIP3 leading to A20 haploinsufficiency cause an early-onset autoinflammatory disease. Nat Genet 2016;48:67–73. [PubMed: 26642243]
52. Lalaoui N, Masters SL. Monogenic disorders of the TNF signalling pathway. Nat Rev Rheumatol 2026;22:8–25. [PubMed: 41381726]
53. Mendell JT, Sharifi NA, Meyers JL, et al. Nonsense surveillance regulates expression of diverse classes of mammalian transcripts and mutes genomic noise. Nat Genet 2004;36:1073–8. [PubMed: 15448691]
54. Zhang J, Webster JD, Dugger DL, et al. Ubiquitin Ligases cIAP1 and cIAP2 Limit Cell Death to Prevent Inflammation. Cell Rep 2019;27:2679–2689 e3. [PubMed: 31141691]
55. Weisel K, Scott N, Berger S, et al. A randomised, placebo-controlled study of RIPK1 inhibitor GSK2982772 in patients with active ulcerative colitis. BMJ Open Gastroenterol 2021;8.
56. Weisel K, Scott NE, Tompson DJ, et al. Randomized clinical study of safety, pharmacokinetics, and pharmacodynamics of RIPK1 inhibitor GSK2982772 in healthy volunteers. Pharmacol Res Perspect 2017;5.
57. Harris PA, Berger SB, Jeong JU, et al. Discovery of a First-in-Class Receptor Interacting Protein 1 (RIP1) Kinase Specific Clinical Candidate (GSK2982772) for the Treatment of Inflammatory Diseases. J Med Chem 2017;60:1247–1261. [PubMed: 28151659]
58. Jones NS, Kshirsagar S, Mohanan V, et al. A phase I, randomized, ascending-dose study to assess safety, pharmacokinetics, and activity of GDC-8264, a RIP1 inhibitor, in healthy volunteers. Clin Transl Sci 2023;16:1997–2009. [PubMed: 37596814]

BACKGROUND AND CONTEXT:

In rare cases, Crohn's Disease (CD) can result from pathogenic variants in genes encoding regulators of Tumor Necrosis Factor, a key driver of intestinal inflammation.

NEW FINDINGS:

We describe 14 patients from 10 independent families with pediatric- and adult-onset CD carrying pathogenic *BIRC3* (encoding cIAP2) variants. This novel form of monogenic IBD leads to dysregulated RIPK1-dependent TNF signaling in intestinal epithelial cells.

LIMITATIONS:

These studies primarily focused on the role of cIAP2 in regulation of RIPK1 and intestinal epithelial cell homeostasis; however, cIAP2 deficiency may also contribute to disease pathogenesis through functions in non-epithelial cells.

CLINICAL RESEARCH RELEVANCE:

This study highlights the therapeutic potential of targeting dysregulated cell death pathways through RIPK1 inhibition in not only patients with *BIRC3*-deficiency but also those with TNF-related forms of monogenic CD, and potentially in a subset of polygenic CD characterized by similar transcriptional profiles.

BASIC RESEARCH RELEVANCE:

Functional studies using human iPSC-derived intestinal organoids, animal models, and cell lines showed that cIAP2 deficiency resulted in dysregulated RIPK1-dependent signaling in the intestinal epithelial and cell death. Overall, reduced cIAP2 expression was effectively mimicking chronic TNF stimulation leading to the development of Crohn's Disease.

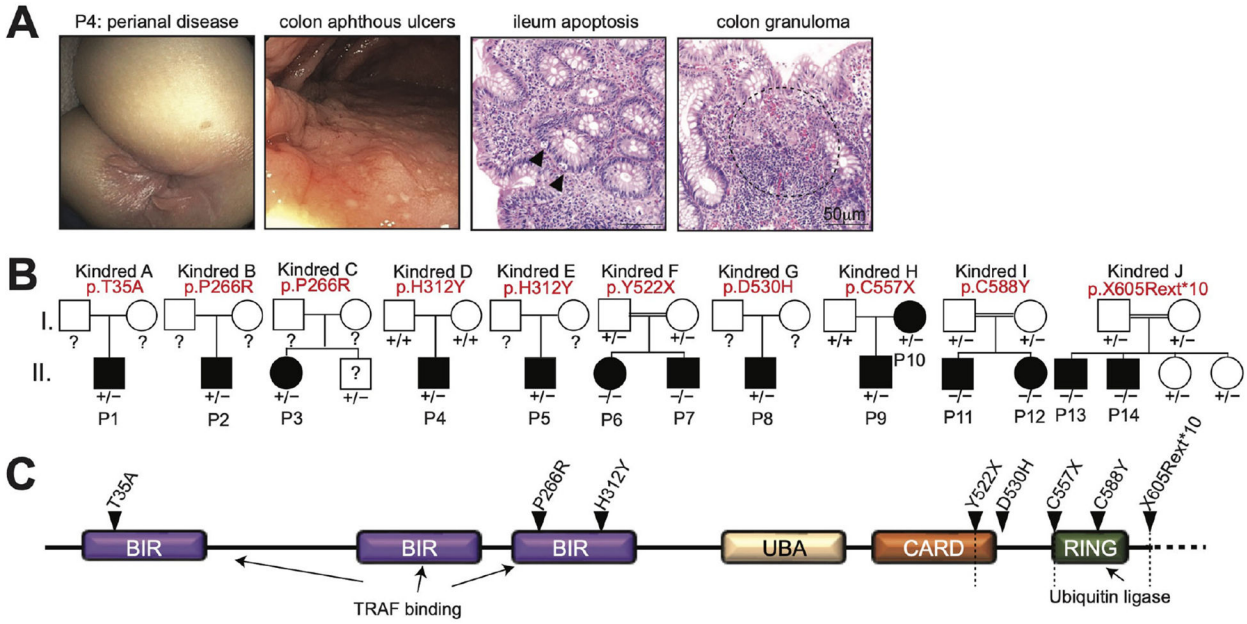

Figure 1. Clinical Features and Genetics Studies of BIRC3-Deficiency

(A) Clinical phenotype of Index patient 4 showing perianal disease (left), aphthous ulcers (middle), and H&E-stained ileal sections showing apoptosis (black arrows, middle), and ileal granuloma (dashed circles) with plasmacytosis (right).

(B) Pedigrees of the kindreds. Circles represent female and squares represent male members. Filled shapes represent the CD phenotype. '+' wildtype, '-' variant, '?' genotype and phenotype unknown.

(C) Structure of the cIAP2 protein indicating the position of patient variants.

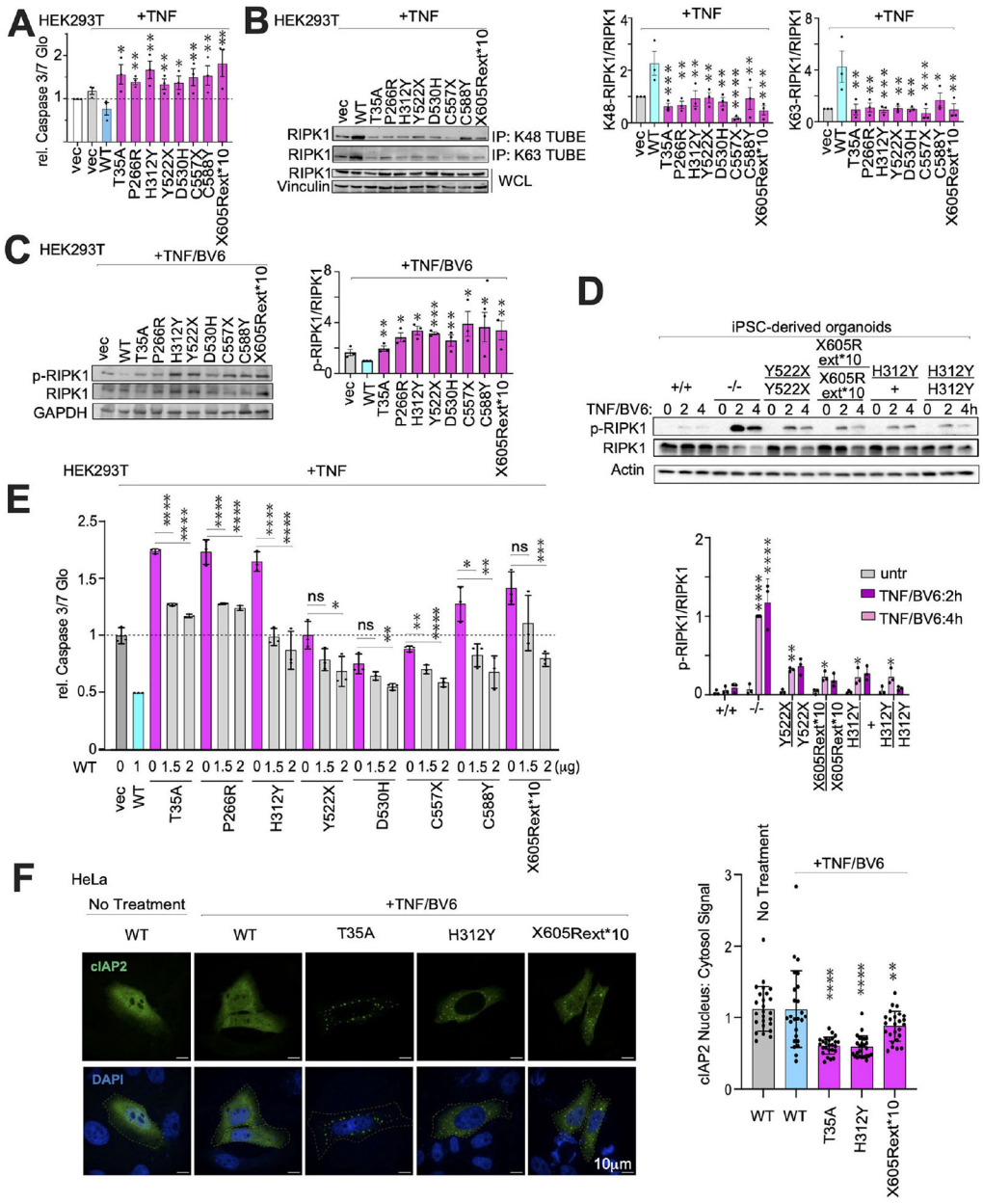

Figure 2. Functional Studies of BIRC3-Deficiency

(A) Caspase3/7 activity assay of overexpressed cIAP2 constructs in HEK293T cells with or without TNF stimulation. (n = 3 biological replicates. Error bars: mean ± SE. Unpaired t test, *p < 0.05, **p<0.01)

(B) K48 and K63 TUBE assays and quantification of RIPK1 ubiquitination in HEK293T cells overexpressing cIAP2 variants after 2 h TNF stimulation. (n = 3 biological replicates; mean ± SE; One-way ANOVA, *p < 0.05, **p < 0.01, ***p < 0.001, ****p < 0.0001)

(C) Western blot assays and quantification of RIPK1 Ser166 phosphorylation in HEK293T cells overexpressing cIAP2 variants after 6 h TNF/BV6 stimulation. (n = 3 biological replicates; mean ± SE; unpaired t test, *p < 0.05, **p < 0.01, ***p < 0.001)

(D) Western blot assays and quantification of serine 166 phosphorylated RIPK1 in human iPSC-derived organoids following TNF/BV6 treatment. (n = 3 biological replicates. Error bars: mean ± SD. One-way ANOVA, *p < 0.05, **p < 0.01, ***p<0.0001)

(E) Caspase-3/7 activity assay of eight patient-derived cIAP2 variants co-transfected with increasing doses of WT cIAP2 in HEK293T cells after TNF stimulation. (n = 3 biological replicates. Error bars: mean ± SE. One-way ANOVA with multiple comparisons, ns>0.05, *p < 0.05, **p < 0.01, ***p<0.001, ****p<0.0001)

(F) Immunofluorescence assay of HeLa cells overexpressing cIAP2 variants and stimulated with TNF/BV6 for 6 hours. Quantitative analysis of cIAP2 by fluorescence intensity in nucleus/cytoplasm. Green: cIAP2; Blue: DAPI, Scale bar: 10μm. Each data point represent a field (>2 cells per field. 25 fields in total). (n=3 biological replicates. Error bars: mean ± SD. Two-way ANOVA. ****p < 0.0001, **p < 0.01)

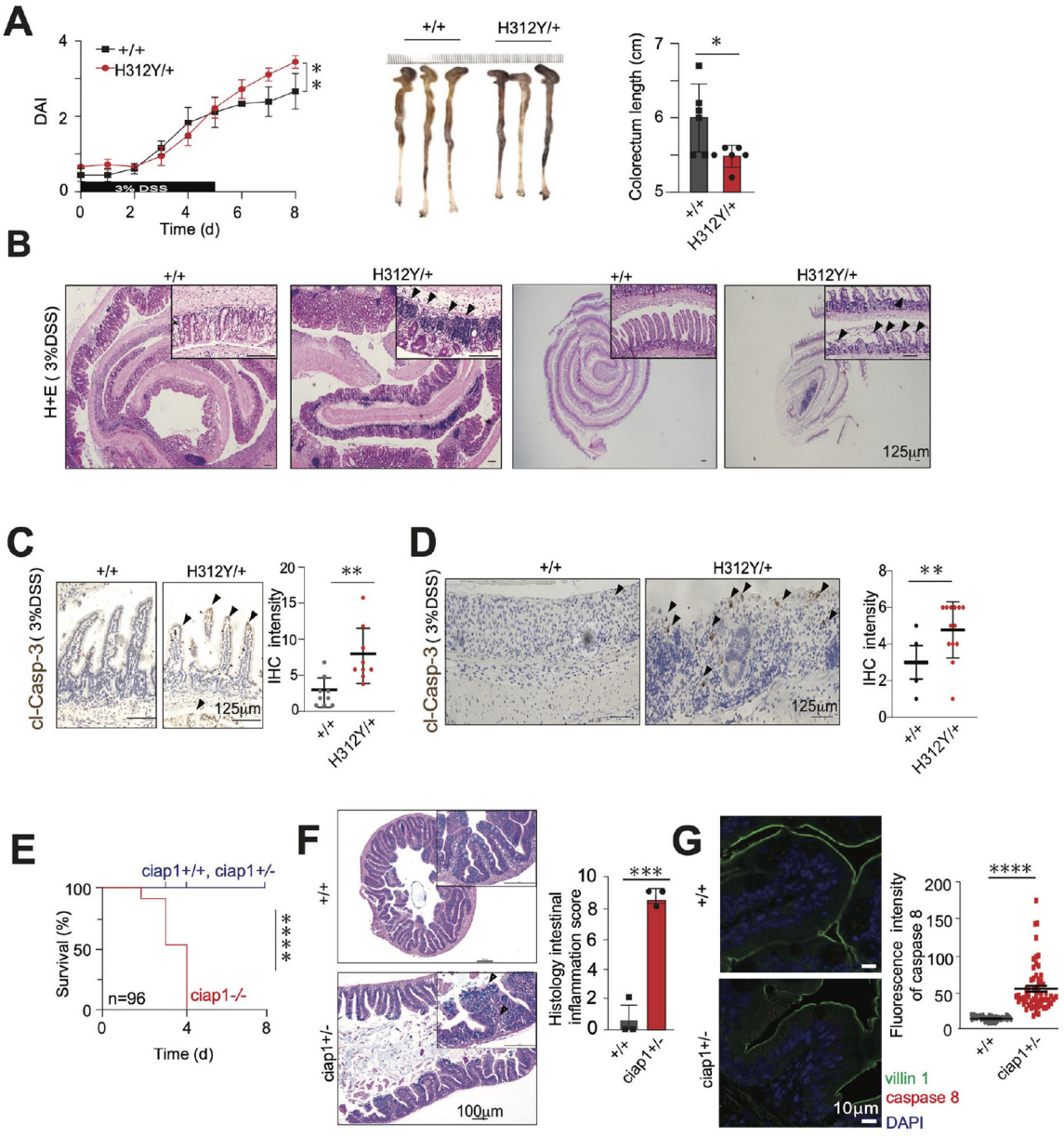

Figure 3. Animal Studies of BIRC3-Deficiency

(A) Disease Activity Index (DAI) and gross morphology of cIAP2$^{+/+}$ and cIAP2$^{H312Y/+}$ mice.

(B) Swiss-roll showing H&E-stained colon (left two panels) or small intestine (right two panels) sections.

(**C-D**) Immunohistochemistry of small intestine **(C)** and colon (**D**) showing cleaved CASPASE-3 (black arrows). cIAP2 $^{+/+}$ (n = 6) and cIAP2$^{H312Y/+}$ (n = 6) 3% DSS–treated mice. The IHC quantification was performed using nine distinct fields of view per group. (Error bars: mean ± SE. Unpaired t test, **p < 0.01)

(E) Kaplan–Meier survival curve of ciap1$^{+/+}$ (n = 25), ciap1$^{-/+}$ (n = 47), and ciap1$^{-/-}$ (n = 24) zebrafish. (Total n = 96, log-rank Mantel–Cox test, ****p < 0.0001)

(F) H&E-stained mid-intestine sections of zebrafish at 1.5 years. (n = 3. Error bars: mean ± SE. Unpaired *t* test, ***$p < 0.001$)

(**G**) Immunofluorescence staining of adult zebrafish intestinal sections with caspase-8 (red), villin 1 (green) and DAPI (blue). (For each sample, 20 enterocytes were analyzed (n = 3). Error bars: mean ± SE. Twotailed Welch's t-test, ****$p < 0.0001$)

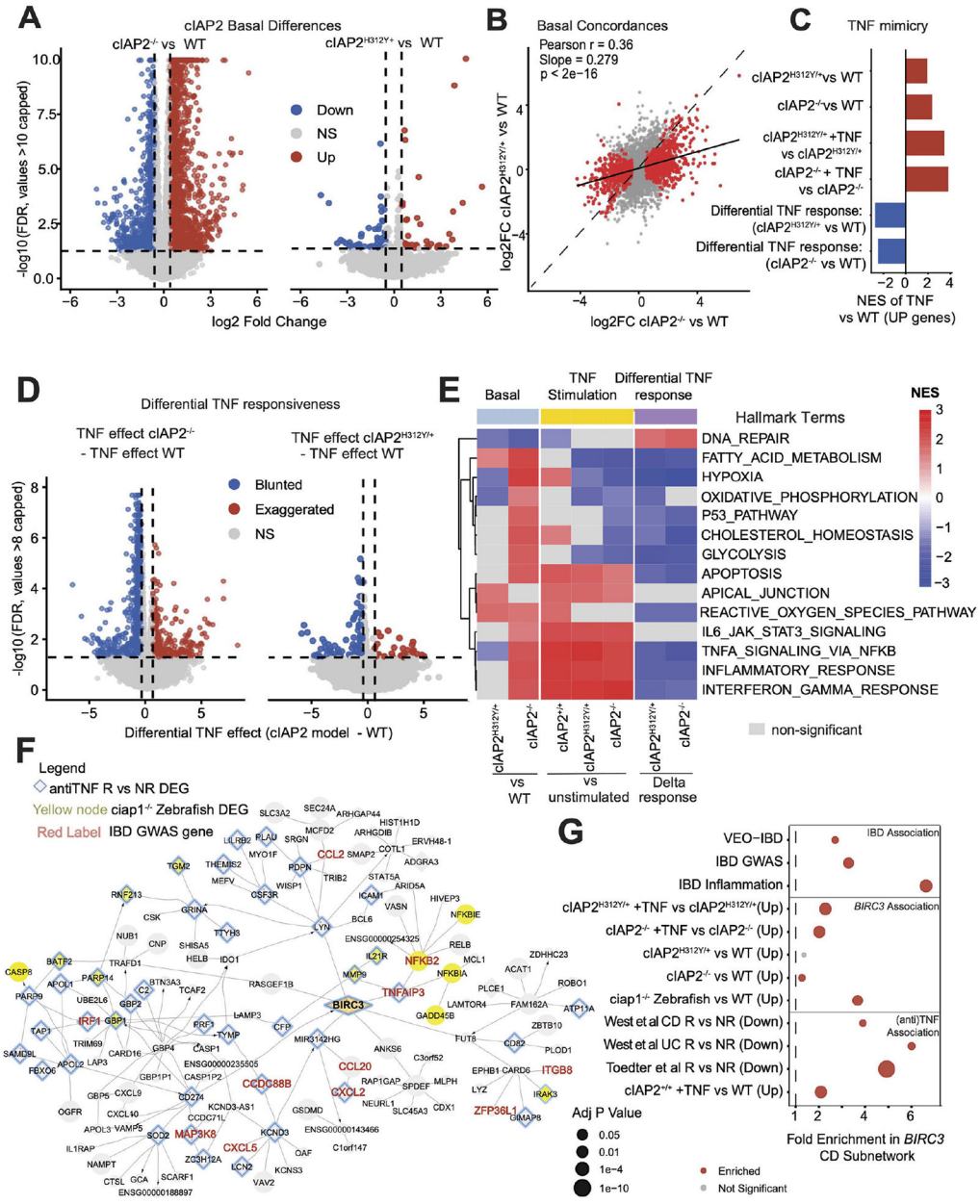

Figure 4. Integrative molecular analysis demonstrates the impact of reduced or absent *BIRC3* expression.

(**A**) Basal transcriptional differences. Volcano plots showing differential gene expression in unstimulated cIAP2$^{-/-}$ and cIAP2$^{H312Y/+}$ mouse intestinal organoids compared to wildtype (WT). cIAP2 deficiency induces a broad inflammatory transcriptional program at baseline, with a stronger magnitude in knockout (cIAP2$^{-/-}$) compared to heterozygous (cIAP2$^{H312Y/+}$) organoids. Dashed vertical lines denote log2 fold-change thresholds; horizontal dashed lines denote FDR cutoff.

(**B**) Basal concordance analysis. Genome-wide log2 fold changes between cIAP2$^{-/-}$ and cIAP2 $^{H312Y/+}$ organoids demonstrated significant positive correlation (Pearson r = 0.36, P < 2×10^{-16}). Linear regression across all genes yielded a slope of 0.28, indicating that

heterozygous organoids retain approximately 28% of the transcriptional amplitude observed in knockout organoids. Among genes significantly dysregulated in cIAP2$^{-/-}$ organoids (red), directional concordance was stronger ($r = 0.53$, $P < 2\times10^{-16}$), with a similar attenuation slope (~0.27).

(**C**) TNF mimicry. Gene set enrichment analysis (GSEA) using TNF-induced WT mouse organoid upregulated genes demonstrates that both cIAP2$^{-/-}$ and cIAP2$^{H312Y/+}$ mouse organoids partially recapitulate TNF-responsive programs in the absence of stimulation. Positive (Red) normalized enrichment scores (NES) indicate constitutive activation of TNF-associated pathways, while interaction terms indicating differential TNF response and defined as TNF effect in cIAP2 model vs TNF effect in control organoids, show attenuation (blue) relative to WT. Ranking metric was t statistic and all assessments FDR <0.05 (Table ST4).

(**D**) Differential TNF responsiveness (interaction analysis). Volcano plots depicting the interaction term, or differential TNF response defined as the change in TNF response in mutant organoids relative to WT. (i.e., ΔTNF_mutant - Δ TNF_WT). Both models show a predominantly blunted TNF response (blue colouring), indicating impaired dynamic adaptation to TNF stimulation.

(E) Hallmark pathway analysis. Heatmap of Hallmark gene set enrichment analysis (GSEA) across basal, TNF-stimulated (+ or – TNF), and interaction (genotype: TNF) conditions. A subset of pathways is shown with intensity and colouring representing either positive (red) or negative (blue) normalized enrichment scores (NES). Ranking statistic was t-statistic and only significant pathway terms show NES with grey colouring indicating non-significant enrichment. Full results in Table ST5. Note negative NES for differential TNF response gene rankings indicates pathways that are attenuated or amplified.

(F) A *BIRC3* centric gene regulatory subnetwork was generated by querying *BIRC3* plus 4 path lengths in a Bayesian network of ~8000 genes generated using transcriptional profiles of colonic biopsies from a cohort of adult CD patients. Nodes are colored yellow if the gene was identified as differentially expressed in the ciap$^{-/-}$ zebrafish model; outlined in blue if identified as a gene reported as differentially expressed between anti-TNF responders and non-responders (NR). Red text coloring indicates an IBD GWAS gene. Edges are directed and represent statistically inferred causal regulatory relationships.

(G) The fold enrichment for the overlap between various genesets and the *BIRC3* centric subnetwork genes described in C. Size of dots represent the level of significance (as -log10 BH-adjusted Fisher Exact Test pvalue). Genesets are categorized according to their informing on IBD association (where IBD Inf = DEGs in Inflamed vs uninflamed human IBD mucosa samples); IBD GWAS and known very early onset IBD genes; or cIAP2 association (DEGs from various cIAP perturbation models) and anti-TNF association (DEGs from cIAP2$^{+/+}$ TNF vs cIAP2$^{+/+}$ and published genesets associated with anti-TNF response in UC and CD).

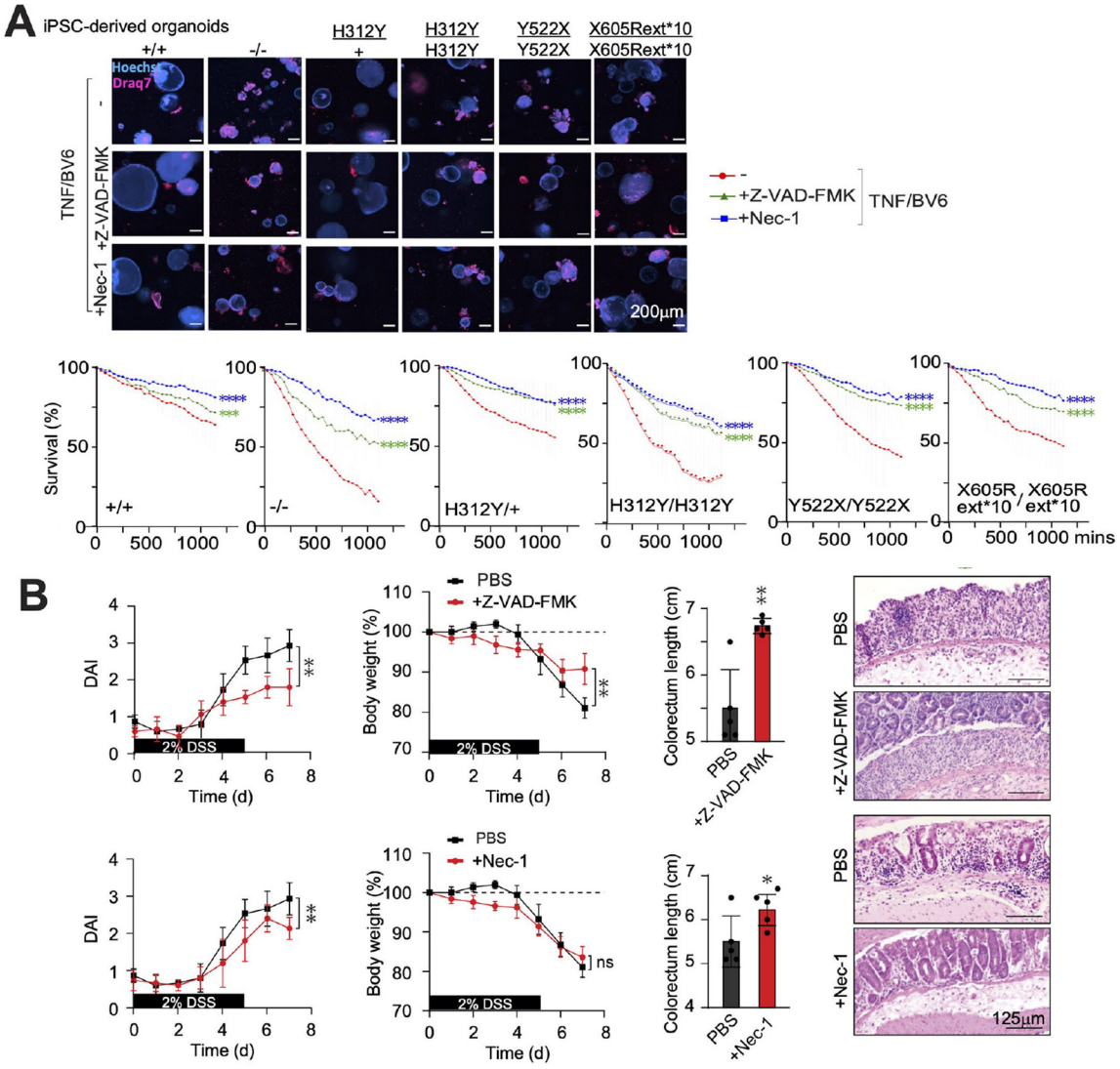

Figure 5. Treatment of BIRC3-Deficiency

(A) Live-cell immunofluorescence assay and quantitative analysis of TNF/BV6-induced cell death in human iPSC-derived intestinal organoids, and the effects of Z-VAD-FMK and Nec-1 rescue. Blue: Hoechst; Red: Draq7, Scale bar: 200 μm. (n = 4 biological replicates. Error bars: mean ± SD. Two-way ANOVA, ****p < 0.0001)

(B) Mice were treated with 5 days of 2% DSS and 3 days of water received either PBS (n = 5), Z-VADFMK (3mg/kg) (n = 5) (top) or Nec-1 (1.5 mg/kg) (n = 5) (bottom). Measurements included body weight change, Disease Activity Index (DAI), colon length change, and H&E staining. Statistical analyses were performed at the predefined experimental endpoint. (Error bars: mean ± SE. Unpaired t-test, ns p > 0.05, *p < 0.05, **p < 0.01)

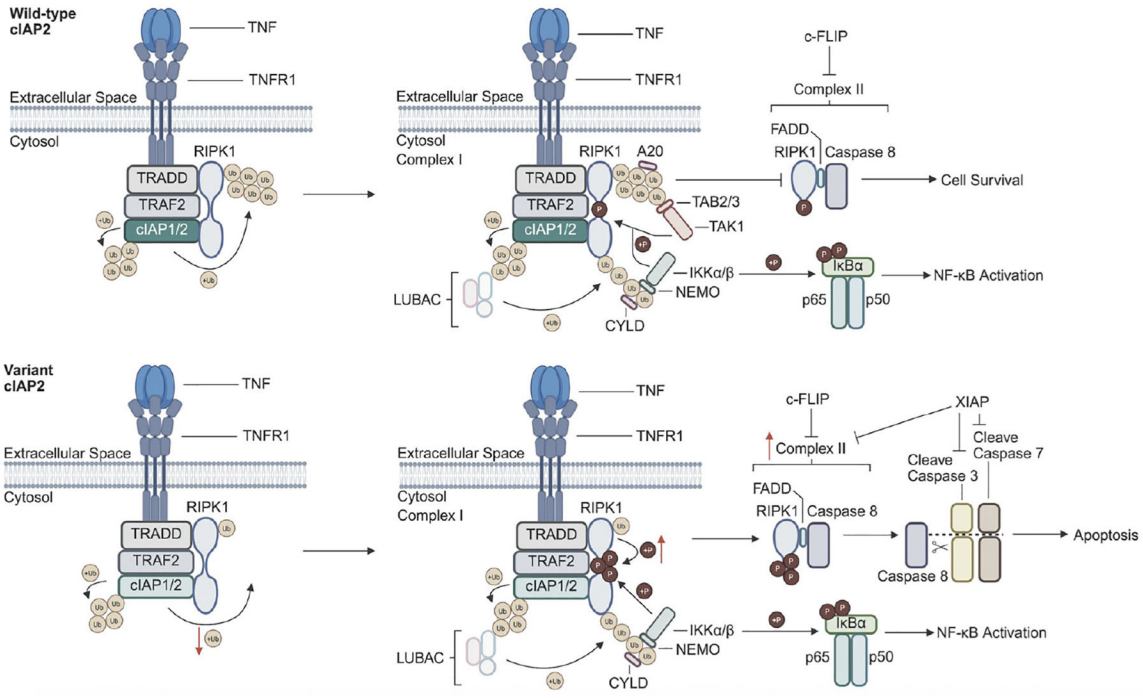

Figure 6. cIAP2 Signaling Pathway

Schematic model illustrating cIAP2 signaling. Wild-type cIAP2 enhances TNF-induced RIPK1 ubiquitination while limiting its phosphorylation, thereby suppressing the formation of active Complex II and promoting cell survival. In contrast, cIAP2 variants fail to regulate RIPK1 ubiquitination, which leads to increased autophosphorylation. As a result, active complex II will further cleave caspases 3 and 7, leading to cell apoptosis.

Table 1.

BIRC3 genetic variant characteristics and patient CD phenotype and treatment.

Patient Number	P1	P2	P3	P4	P5	P6	P7	P8	P9	P10	P11	P12	P13	P14
Kindred	A	B	C	D	E	F		G	H		I		J	
Amino Acid Position	**p.T35A**	**p.P266R**		**p.H312Y**		**p.Y522X**		**p.D530H**	**p.C557X**		**p.C588Y**		**p.X605Rext*10**	
Nucleotide Position	c.103A>G	c.797C>G		c.934C>T		c.1566T>A		c.1588G>C	c.1671T>A		c.1763G>A		c.1813T>C	
Allele Status	hetero	hetero		hetero		homo		hetero	hetero		homo		homo	
Variant Annotation														
Chromosome	11	11		11		11		11	11		11		11	
position (GRCh38)	102324612	102325306		102325546		102336207		102336768	102336958		102337050		102337100	
dbSNP151	-	rs201026275		-		-		rs749715948	rs774719063		-		-	
position (GRCh37)	102195343	102196037		102196277		102206938		102207499	102207689		102207781		102207831	
gnomADv4 maf	novel	0.00002975		novel		novel		6.22E-07	6.23E-07		novel		novel	
COSMIC	-	-		1		-		-	-		-		-	
CADD_phred (GRCh37-v1.6)	25.3	25.0		27.1		34.0		22.2	36.0		27.0		16.1	
Clinical Presentation														
IBD Classification	CD	CD	CD	CD	CD	CD	CD	CD	CD	CD	CD	CD	CD	CD
Age of IBD Onset (years)	20	17	3	4	12	0.6	0.9	12	0.8	31	1	0.8	0.1	0.5
Sex (M=male, F=female)	M	M	M	M	M	F	F	M	M	F	F	F	M	M
Consanguinity	n/a	n/a	no	n/a	n/a	yes		n/a	no		yes		yes	
Disease Location	n/a	ileo-colonic	ileo-colonic	ileo-colonic	ileo-colonic	ileo-colonic	ileo-colonic, esophagus	ileo-colonic	ileo-colonic	colonic	ileo-colonic	colonic	colonic	colonic
Stricturing	n/a	yes	yes	no	n/a	no	no	no	no	no	no	no	no	no
Perianal Disease	n/a	yes	yes	yes	yes	no	no	yes	no	no	no	no	no	no

Gastroenterology. Author manuscript; available in PMC 2026 July 07.

Fever	n/a	no	no	yes	n/a	yes	no	n/a	n/a	n/a	yes	yes	no	no
Skin Inflammation	n/a	no	no	no	n/a	yes	no	n/a	yes	n/a	no	no	no	no
Joint Inflammation	n/a	no	no	no	n/a	no	no	n/a	yes	n/a	no	no	no	yes
Recurrent Infections	n/a	no	no	no	n/a	no	no	n/a	n/a	n/a	yes	yes	no	no
Surgery and Therapy (chronological order first used)	n/a	n/a	colectomy, abdominoperineal resection 5-ASA, AZA, IFX, ADA	IFX + MTX	n/a	colectomy IFX	5-ASA	n/a	n/a	n/a	VDZ + AZA	VDZ + AZA	UST	UST
ACMG Classification	LP	VUS		LP		LP		LP	LP		LP		LP	

NB: systemic granulomatous disease (liver, lymph nodes)

Abbreviations: n/a - not available, CD - Crohn's Disease, LP - Likely Pathogenic, VUS - Variant of Unknown Significance, IFX - infliximab, MTX - methotrexate, ASA - acetylsalicylic acid, VDZ - vedolizumab, AZA - azathioprine, UST – ustekinumab, dash (–) indicates no data.